International Journal of Pharmaceutics 589 (2020) 119840

Contents lists available at ScienceDirect

International Journal of Pharmaceutics

journal homepage: www.elsevier.com/locate/ijpharm

Buclizine crystal forms: First Structural Determinations, counter-ion stoichiometry, hydration, and physicochemical properties of pharmaceutical relevance

Monalisa Bitencourt[a,c], Olimpia Maria Martins Santos Viana[a], Andre Luiz Machado Viana[a], Jennifer Tavares Jacon Freitas[a], Cristiane Cabral de Melo[a,b,*], Antonio Carlos Doriguetto[a,b,*]

[a] Faculty of Pharmaceutical Sciences, Federal University of Alfenas, Rua Gabriel Monteiro da Silva, 701 Alfenas, Minas Gerais 37130-001, Brazil
[b] Institute of Chemistry, Federal University of Alfenas, Rua Gabriel Monteiro da Silva, 701, Alfenas, Minas Gerais 37130-001, Brazil
[c] Novartis Pharmanalytica AS, Via Serafino Balestra, 31, 6600 Locarno, Switzerland

ARTICLE INFO

Keywords:
Buclizine
Counter-ion stoichiometry
Hydration
Equilibrium solubility
Dissolution profile
Structure determination
Crystal engineering

ABSTRACT

Buclizine (BCZ) is a chiral synthetic piperazine derivative which has antihistaminic, anti-muscarinic and antiemetic properties, and has been reintroduced as an appetite stimulant, especially for pediatric patients. Structural information about this drug, as well as other buclizine crystalline forms (solvates, salts and co-crystals) including the BCZ free-base (BCZ-FB), is non-existent. Here, we present for the first time the crystal structure of the monohydrochloride monohydrate salt of BCZ ($BCZHCl{\cdot}H_2O$), and of its anhydrous form, BCZHCl. Interestingly, $BCZHCl{\cdot}H_2O$ was obtained by recrystallization from the raw material ($BCZH_2Cl_2$) in ethanol:water solution showing that BCZ anhydrous dihydrochloride salt changes easily to a monohydrochloride monohydrate salt modification, which raise concerns about formulation quality control. $BCZHCl{\cdot}H_2O$ and BCZHCl crystallize in the orthorhombic space groups ($Pna2_1$ and $Pca2_1$) belonging to the mm2 point group and are thus classified as non-centrosymmetric achiral structures (NA). Intuitively, we expect these salts to crystallize in a space group with a center of symmetry, since less than 5% of the known racemic compounds crystallize in the NA type. The crystal structures of $BCZH_2Cl_2$ and BCZ-FB were not determined, but their existence was verified by other techniques (chloride ion analysis, PXRD, HPLC, FT-IR, DSC, TGA) and by comparison of the obtained results with those found for BCZHCl. Additionally, we have also performed an evaluation of the equilibrium solubility (at six different aqueous media) and the dissolution profile of the BCZHCl salt compared to the raw material and BCZ-FB. Different equilibrium solubility values were found comparing the three forms in acidic and neutral pH ranges and all of them were insoluble at pH $>$ 7.0. Moreover, tablets prepared with $BCZH_2Cl_2$, BCZHCl or BCZ-FB show significant differences in terms of dissolution profile.

1. Introduction

Buclizine (BCZ), (R,S)-1-(4-*tert*-butybenzyl)-4-(4-chlorobenzhydryl) piperazine, is a sedating antihistaminic drug (Kuminek et al., 2012; Mostafa and Al-Badr, 2011) administered as a syrup and tablets in its dihydrochloride salt modification (Scheme1) under several brand names: Aphilan, Bucladin-S, Buclina, Longifene, Posdel, Postadoxine, Postafen, Postafeno, Softran, Vibazine (Mostafa and Al-Badr, 2011). Structurally, this compound is very similar to other antihistaminic drugs: meclizine, cetirizine, cyclizine and hydroxyzine (Peraman et al., 2015). Due its antiemetic action, BCZ is particularly applied for the treatment of migraine (in combination with other analgesics) and in the prevention of motion sickness (nausea, vomiting), although it has been used in some countries for the man.agement of allergic disorders (Mostafa and Al-Badr, 2011; Conklin and Nesbitt, 1958). Nausea and emesis (or vomiting) are triggered by stimulation of either the chemoreceptor trigger zone (CTZ) or the emesis center in the central nervous system. BCZ acts by binding and blocking the histamine and

Abbreviations: CTZ, Chemoreceptor Trigger Zone; BCS, Biopharmaceutical Classification System; BCZ, Buclizine; BCZ-FB, Buclizine free-base; CSD, Cambridge Structural Database; FDA, Food and Drug Administration; PXRD, Powder X-ray Diffraction; FT-IR, Fourier Transform Infrared; HPLC, High Performance Liquid Chromatography, SCXRD, Single-Crystal X-ray Diffraction; DSC, Differential Scanning Calorimetry; TGA, Thermogravimetric Analysis; $BCZH_2Cl_2$, Buclizine Dihydrochloride; BCZHCl, Buclizine Monohydrochloride

* Corresponding authors at: Institute of Chemistry, Federal University of Alfenas, Rua Gabriel Monteiro da Silva, 701 Alfenas, Minas Gerais 37130-001, Brazil.
E-mail addresses: crisbrizoti@gmail.com (C.C. de Melo), doriguetto@unifal-mg.edu.br (A.C. Doriguetto).

https://doi.org/10.1016/j.ijpharm.2020.119840
Received 11 June 2020; Received in revised form 13 August 2020; Accepted 30 August 2020
Available online 02 September 2020
0378-5173/

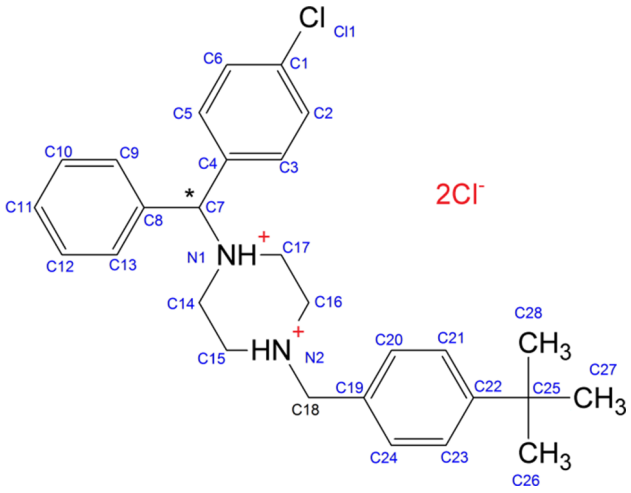

Scheme 1. Molecular Structure of Buclizine Dihydrochloride.

muscarinic receptors in the emesis center, thereby preventing the activation of CTZ and reducing nausea and vomiting (Mostafa and Al-Badr, 2011; Conklin and Nesbitt, 1958; Watcha, 2002). More recently, BCZ has been reintroduced as an appetite stimulant for weight gain in children and adults (Mostafa and Al-Badr, 2011; Babu, 2011). The orexigenic effect is not well understood, but it is thought to be due to its hypoglycemic action.

Even in its saline form (dihydrochloride), as expected in medicine, BCZ is known as a low solubility drug (Mostafa and Al-Badr, 2011), but is not specified as belonging to class II (low solubility and high permeability) or IV (low solubility and low permeability) in the Biopharmaceutical Classification System (BCS). Independently, BCZ is expected to show low dissolution rates due to its low solubility, which often cause limited bioavailability (Yu et al., 2002; Amidon et al, 1995). Especially if the drug is BCS class II, where the limiting step is the drug release from the dosage form and the solubility in the gastrointestinal fluid and not the absorption, its bioavailability would be modulated only by increasing the aqueous solubility (Yu et al., 2002; Amidon et al, 1995).

The definition of drug solubility is based on the highest dose strength of an immediate release product, *i.e.* with no less than 85% of the dose dissolved within 30 min, according to the United States Food and Drug Administration (US-FDA) BCS criteria (FDA, 2017). Therefore, a drug can be considered highly soluble (BCS class I or III) when the highest dose strength is soluble in 250 mL or less of aqueous media over the pH range from 1.0 to 7.5. The volume of 250 mL comes from typical bioequivalence study protocols that prescribe the administration of a drug product to fasting human volunteers with a glass of water (Yu et al., 2002; Amidon et al, 1995).

Since water is the preferential solvent for liquid pharmaceutical formulations, several methods have been developed to improve the solubility of poorly water-soluble drugs including the reduction of particle size, the use of solid dispersions, microemulsions, inclusion complexes (drug-cyclodextrin complexes), co-solvents and salt formers, besides others (Savjani et al., 2012). For acid and basic drugs, salt formation is by far the most appropriate method for increasing solubility and the dissolution rate (Serajuddin, 2007; De Melo et al, 2016; Cruz-Cabeza, 2012).

BCZ free-base is a dibasic molecule with pKa values of 2.12 and 6.55 so can therefore form both mono- and di-salts by protonation of the piperazine nitrogens (ACD/ChemSketch, 2018). Furthermore, it contains a chiral center (C7 atom, Scheme 1), which is being marketed as an equimolar mixture of two different optical isomers or enantiomers. This, in turn, implies that the BCZ raw material as well as the other buclizine crystalline forms recrystallized from it may belong to one of three classes: a conglomerate (a physical mixture of pure enantiomers crystals); a racemic compound (the two enantiomers coexisting in equal quantities in the same crystal); or a pseudoracemate/solid solution (the two enantiomers coexisting in an unordered manner in the same crystal (Mitchell, 1998). Indeed, before this work, such information was unknown due to the lack of X-ray structures available on the Cambridge Structural Database (Allen, 2002). A CSD search revealed no entry for BCZ dihydrochloride salt and other BCZ crystalline forms (solvates, salts and co-crystals), including the BCZ free-base.

In this study, we report the X-ray structures of the monohydrochloride monohydrate salt of BCZ (hereafter BCZHCl·H_2O) and of its anhydrous form (hereafter BCZHCl) for the first time. In contrast to the BCZHCl, which was obtained through the deprotonation of $BCZH_2Cl_2$, BCZHCl·H_2O resulted from the recrystallization of the commercial raw material ($BCZH_2Cl_2$). The mechanism by which this anionic change occurs is unknown, but a chloride ion-selective analysis was employed to determine the authenticity of the powder raw material and the corresponding monohydrochloride BCZ salts (hydrate and anhydrous forms).

Although it has not been possible to determine the X-ray structures of $BCZH_2Cl_2$ and BCZ free-base (hereafter BCZ-FB), their existence was confirmed by Powder X-ray diffraction (PXRD), Fourier Transform Infrared spectroscopy (FT-IR), High Performance Liquid Chromatography (HPLC) analysis, Differential Scanning Calorimetry (DSC) and Thermogravimetric Analysis (TGA) techniques. Additionally, this study also presents an evaluation of the equilibrium solubility (at six different aqueous media) and the dissolution profile of BCZHCl compared to the raw material ($BCZH_2Cl_2$) and BCZ-FB.

2. Experimental section

2.1. Materials and reagents

Anhydrous sodium acetate, acetic acid, phosphoric acid, hydrochloric acid, trihydrated sodium acetate, methanol, potassium hydrogen phosphate, acetonitrile and sodium lauryl sulfate (LSS) from Merck™; sodium hydroxide from Fluka™; chloroform from Synth™; ethanol from Dinâmica™; acetone from Sigma-Aldrich™. Ultrapure water from Milli-Q- Merck-Millipore™. A commercial raw material sample of $BCZH_2Cl_2$ was obtained from D.K. Pharmachem Pvt. Ltd, Mumbai, India. Raw material and all solid forms obtained during the crystal engineering procedures (see section 2.2) were stored at room temperature (25 °C) protected from light and moisture.

2.2. Samples

2.2.1. *Buclizine dihydrochloride* ($BCZH_2Cl_2$)

The raw material (99.2% +/- 0.8 of $BCZH_2Cl_2$ by HPLC analysis) was used as received in the characterization part (API:Cl^- ratio analysis, PXRD, FT-IR TGA and DSC analyses), which confirmed its solid phase identity (See Discussion), and also in the comparative physicochemical studies involving the other two BCZ forms (BCZHCl and BCZ-FB). Interestingly, recrystallization procedures (Beckmann, 2013; Gao et al., 2017) using raw material as a solute resulted in single crystals of BCZHCl·H_2O instead of $BCZH_2Cl_2$ (see 2.2.2). Indeed, attempts either to obtain $BCZH_2Cl_2$ single crystals good enough for a single-crystal X-ray diffraction experiment or to determine the crystal structure of $BCZH_2Cl_2$ from powder X-ray diffraction data were unsuccessful.

2.2.2. *Buclizine monohydrochloride monohydrate (BCZHCl·H_2O).*

To obtain single crystals of BCZHCl·H_2O, 3.0 mg of the raw material were dissolved in 50 mL of an ethanol:water (1:1, v:v) solution at 75 °C. The heated solution was filtered and allowed to reach 25 °C. Then, this solution was transferred to a flask capped with a parafilm layer punctured with small holes. During the evaporation process, the flask was maintained at 8 °C without the direct incidence of light. Needle-shaped crystals of BCZHCl·H_2O were grown after 21 days by slow evaporation

of the solvent (Beckmann, 2013; Gao et al., 2017). The most suitable single crystals were removed from the crystallization solution and storage in coin capsules. To avoid evaporation of the solvent and consequently amorphization of the crystals, they are covered by a thin layer of vegetable oil. The coin capsules were kept at room temperature protected from the light. Attempts to obtain sufficient pure polycrystalline BCZHCl·H_2O for the characterization part and the comparative physicochemical studies were unsuccessful.

2.2.3. Buclizine monohydrochloride (BCZHCl)

To obtain BCZHCl polycrystalline material, 1.0 g of the raw material ($BCZH_2Cl_2$) was solubilized at room temperature (25 °C) in 500 mL of a methanol:water mixture (1:1, v:v). The solution was sonicated for 10 min followed by neutralization with drops of 1.0 mol L^{-1} NaOH solution until it became cloudy, which took place at approximately pH 4.8. As expected, this pH is at the middle of the pH range between the two calculated BCZ pKa values (pKa1 = 2.12 and pKa2 = 6.55, See section 3.3). The solution flask was capped with a parafilm layer (punctured with small holes) and stored without the direct incidence of light. It is important to emphasize that the precipitate formed soon after the $BCZH_2Cl_2$ neutralization was amorphous (Figure S1, Supplementary material). Crystalline BCZHCl without the presence of an amorphous halo in the PXRD experiment was obtained by leaving the precipitate to stand in contact with the stock solution for at least 10 days. In this way, after 13 days, the precipitate on the flask bottom was separated from the solution and dried in a desiccator containing silica for 24 h. The generation of the BCZHCl form was confirmed by PXRD data (See Discussion) and its chemical purity (99.6% +/- 0.3) attested by HPLC analysis. The BCZHCl polycrystalline material was stored without the direct incidence of light for the further analysis. The freshly prepared BCZHCl polycrystalline material was also used in recrystallization procedures in order to grow BCZHCl single-crystals that were good enough for the single crystal X-ray experiment. After several attempts, single-crystals were successfully obtained by vapor diffusion crystallization method (Beckmann, 2013; Gao et al., 2017) as follow: approximately 2.0 mg of the BCZHCl form was dissolved in 0.5 mL of acetone within a small open container (beaker of 10 mL), which was placed in a larger container (vial of 50 mL) containing 2.5 mL of chloroform. The outer container was sealed and the vapor chloroform solution diffusion process into the acetone container was performed at 25 °C. Plate-shaped colorless crystals were obtained after 15 days.

2.2.4. Buclizine free-base (BCZ-FB)

To obtain BCZ-FB polycrystalline material, 1.0 g of the raw material was solubilized at 25 °C in 500 mL of ethanol:water (1:1, v:v) mixture. After sonication for 10 min, 1.0 mol L^{-1} NaOH solution was trickled into the vial until pH 5.8 was reached (optimized value to produce BCZ-FB absent of BCZHCl), which produced a significant amount of a white colloidal precipitate. The remaining procedures were the same as those applied to obtain the polycrystalline $BCZH_2Cl_2$ sample. The generation of BCZ-FB was confirmed by HPLC (chemical purity of 99.5% +/- 0.01), PXRD, IR, DSC, and TGA data (See Discussion). Unfortunately, several attempts using different crystal growth protocols to obtain BCZ-FB single crystals that were good enough for a single-crystal X-ray diffraction experiment were unsuccessful. Attempts to determine the crystal structure of BCZ-FB from powder X-ray diffraction data were also unsuccessful.

2.3. Single crystal X-ray diffraction analysis (SCXRD)

Suitable BCZHCl·H_2O and BCZHCl single-crystals were previously selected for the X-ray measurements. The data collections were performed on an Agilent™ SuperNova diffractometer, equipped with dual source of radiation (Cu and Mo) and an Atlas S2 CCD detector at 293 and 150 K (only for BCZHCl·H_2O crystal). The CrysalisPro software (Agilent, 2010) was used for data collection, unit cell determination, data reduction and multi-scan method absorption correction. The structures were solved by direct methods and refined by full-matrix least squares on F^2 using the SHELXL-2018/3 software (Sheldrick, 2015). All non-hydrogen atoms were found from the electronic density map constructed by Fourier synthesis and refined with anisotropic thermal parameters. All hydrogen atoms (with exception of the water hydrogen atoms) were placed in idealized positions in a riding model with fixed C—H (or N—H) bond lengths of 0.98, 0.93, 0.96, 0.97 and 0.98 Å for the amino, aromatic, methyl, methylene and methine groups, respectively. The isotropic thermal parameters of all hydrogens (except the water hydrogens) depended on the equivalent isotropic thermal displacements of the atoms bonded to them [Uiso(H) = 1.2Ueq(N-amino, C-aromatic, C-methylene, C-methine) or 1.5Ueq(C-methyl)]. In the low temperature (150 K) structure of BCZHCl·H_2O, electron density peaks corresponding to positions of the water hydrogen atoms were identified and assigned at approximately 1 Å from the oxygen atom (O1). Their positions (distances) nonetheless were restrained using DFIX (O1-H1/O1-H2 = 0.84(2) Å) and DANG (H1-H2 = 1.34(4) Å) instructions (Sheldrick, 2015), with Uiso(H1/H2) values = 1.5Ueq (O1). For the room temperature (293 K) dataset, one of the water hydrogens is shared between the water oxygen and the amino nitrogen (assigned in accordance with residual peaks without distance restraints), giving a final model after occupancy refinement of 23% water/77% buclizine monohydrochloride and 77% hydroxide ion/23% buclizine dihydrochloride. As previously observed for BCZ analogous structures (Deb et al, 2015; Mohanty et al., 2015; Song et al, 2012), the chlorine atom (Cl1) of 1-[(4-chlorophenyl)(phenyl)methyl]piperazinediium moiety was disordered over the two-symmetric benzene carbon atoms (C1 and C11, Scheme 1). In all structures, the chlorine atom was disordered over the Cl1-C1/Cl1-C11′ positions, with refined site-occupation factors of 0.835(4)/0.165(4) (BCZHCl), 0.889(6)/0.111(6) (BCZHCl·H_2O at 150 K) and 0.940(4)/0.060(4) (BCZHCl·H_2O at 293 K). The occupancy factors were assigned using the free variables and restraining the sum of them equal to 1.000 (FVAR SHELXL-2018/3 instruction) (Sheldrick, 2015). The Flack parameter for BCZHCl dataset (Cu radiation dataset) was reliably refined (Flack, 2003, 1983; Cianci et al, 2005; Parsons and Flack, 2004) to 0.04(3) ((R)-isomer) using the BASF/TWIN SHELXL-2018/3 instruction (Sheldrick, 2015). Refinement of the Flack parameter for BCZHCl·H_2O datasets (both Mo radiation datasets) at 150 K and 293 K was 0.08(16) and −0.03(10) respectively, giving an inconclusive indication of the absolute structure, since the standard uncertainty values are above 0.10. A favorable outcome was obtained from the Bijvoet analysis reported by Hooft et al. (Hooft et al., 2008, 2010) and implemented in the PLATON program (Spek, 2009). However, due to the low Friedel coverage, this analysis was inconclusive for the low temperature dataset. The probability that the (R)-isomer had been correctly assigned was 1.00 for either P2 (probability assuming two possibilities, *i.e.* one enantiomer or the other) or P3 (probability assuming three possibilities, including the two possible enantiomers plus the third option of a racemic twin). The resulting value of the Hooft parameter y was 0.03(3). Therefore, since BCZHCl and BCZHCl·H_2O were solved respectively in the *P*na2_1 and *P*c$a2_1$ polar space groups (non-centrosymmetric space group containing mirror planes), both are racemic crystals, so it obviously makes no sense to establish the BCZ absolute configuration from the absolute structure. The MERCURY (version 3.9) software program was used for crystallographic analysis and artwork representations, in which the disorder was omitted for the sake of clarity, *i.e.* only the chlorine atom with highest site-occupation factors -linked to C1- was included. The crystal data and details of data collection and refinement are shown in Table 1. CCDC 1,912,183 (BCZHCl), CCDC 1,912,184 (BCZHCl·H_2O at 293 K) and CCDC 2,008,948 (BCZHCl·H_2O at 150 K) contain the supplementary crystallographic data for this paper. The data can be obtained free of charge from The Cambridge Crystallographic Data Centre (CCDC) via www.ccdc.cam.ac.uk/getstructures. (Allen, 2002).

Table 1
Crystal data and structure refinement parameters for BCZ salts.

	BCZHCl·H_2O	BCZHCl·H_2O	BCZHCl
Formula	$C_{28}H_{36}Cl_2N_2O$	$C_{28}H_{36}Cl_2N_2O$	$C_{28}H_{34}Cl_2N_2$
Formula weight (g mol^{-1})	487.49	487.49	469.47
Temperature (K)	150(2)	293(2)	293(2)
Wavelength (Å)	0.71073	0.71073	1.54184
Crystal System	Orthorhombic	Orthorhombic	Orthorhombic
Space group	$Pna2_1$	$Pna2_1$	$Pca2_1$
Unit cell dimensions (Å)	a = 25.018(2)	a = 25.156(2)	a = 11.6629(3)
	b = 15.6230(11)	b = 15.7503(15)	b = 10.5092(3)
	c = 6.9000(6)	c = 6.9637(6)	c = 21.0777(7)
Volume ($Å^3$)	2697.0(4)	2759.2(4)	2583.45(13)
Z, Ź	4, 1	4, 1	4, 1
Calc. Density (g cm^{-3})	1.201	1.174	1.207
Absorp. coefficient (mm^{-1})	0.263	0.257	2.379
F(000)	1040	1040	1000
Data collect. θ range (°)	2.732 to 29.729	3.199 to 29.712	4.195 to 73.451
Index ranges	$-34 \le h \le 33$	$-31 \le h \le 29$	$14 \le h \le 14$
	$-16 \le k \le 19$	$-21 \le k \le 13$	$-13 \le k \le 8$
	$-7 \le l \le 9$	$-9 \le l \le 6$	$-25 \le l \le 26$
Reflections collected	20,478	12,637	22,462
Independent reflections	5957 [$R_{(int)}$ = 0.0714]	5510 [$R_{(int)}$ = 0.0408]	5030 [$R_{(int)}$ = 0.0589]
Completeness to $\theta_{max.}$ (%)	89.0	97.3	100.0
Data/restraints/parameters	5957/4/318	5510/1/313	5030/1/295
Goodness-of-fit on F^2	1.119	1.068	1.079
Final R indices [I > 2σ(I)]	R1 = 0.0898, wR2 = 0.1997	R1 = 0.0603, wR2 = 0.1192	R1 = 0.0649, wR2 = 0.1830
R indices (all data)	R1 = 0.1220, wR2 = 0.2199	R1 = 0.1010, wR2 = 0.1366	R1 = 0.0685, wR2 = 0.1871
Absolute structure parameter	0.08(16)	−0.02(10)	0.04(3)
Largest diff. peak and hole ($e.Å^{-3}$)	0.83 and −0.33	0.22 and −0.15	0.47 and −0.40

2.4. Powder X-ray diffraction analysis (PXRD)

The PXRD analyses were performed at room temperature (293 K) on a Rigaku™ (Japan) Ultima IV X-ray diffractometer using the CuKα radiation (λ = 1.5418 Å) generated in a sealed tube energized at a voltage of 40 kV and current of 30 mA. For the experimental analysis, samples were placed on the standard sample holder and then scanned continuously. The data were collected with a 2θ step size of 0.02°, scan speed of 1° 2θ min^{-1} and angular range from 3° to 35° in 2θ.

2.5. Thermal analysis.

Differential scanning calorimetry (DSC) experiments were obtained under a dynamic atmosphere of nitrogen (50 mL min^{-1}) with a heat flow of 10 °C min^{-1}, between 30 and 260 °C, on a NEZSTCH™ DSC, model DSC Syrius 3500 (Germain). Approximately 3 mg of sample was placed in an open aluminum crucible. The instrument was calibrated with an indium standard. Thermogravimetric analysis (TGA) and Differential thermal analysis (DTA) curves were performed using about 3 mg of sample in open aluminum crucibles, on Thermobalance SII Nano Technology™, model TGA/DTA-7300 (Japan). The curves were obtained under a dynamic atmosphere of nitrogen flow (50 mL min^{-1}), with a heat flow of 10 °C min^{-1}, between 30 and 500 °C.

2.6. Fourier transform infrared (FT-IR) spectroscopy

The spectra were recorded on a Shimadzu™ spectrophotometer, model Prestige-21 (Japan), using KBr pellets. The transmittance mode data were collected at 25 °C: resolution 4 cm^{-1}, 64 scans, range of 4000–400 cm^{-1}.

2.7. Optical rotation measurements

0.2 g of $BCZH_2Cl_2$ (raw material) was solubilized at 25 °C in 500 mL of methanol:water (1:1, v:v) mixture. Optical rotation measurements were performed on a Quimis™ automatic polarimeter, model Q-760 M (Brazil), confirming that the raw material bulk is a racemic mixture.

2.8. Residual chloride quantification

A mass of 100 mg of BCZ-FB, BCZHCl, BCZHCl·H2O and $BCZH_2Cl_2$ (raw material) was separately weighed, transferred to a 5 mL volumetric flask and solubilized in chloroform p.a. (Anidrol, Brazil). Liquid-liquid extraction was performed by adding 5 mL of water to a 25 mL falcon centrifuge tube and centrifuging this for 10 min at 3000 g. The aqueous part was separated and quantified in a spectrophotometer (Shimadzu™, Japan, model UV-1800), by colorimetric reaction using a commercial kit (mercury and iron thiocyanate) (Labtest Diagnóstica, Brazil), according to the manufacturer's instructions. As expected, the free base did not quantify residual chloride, the BCZHCl and BCZHCl·H_2O forms showed similar residual chloride values and the $BCZH_2Cl_2$ showed twice the residual chloride value compared with these forms, confirming the nominal API:counter-ion ratios (1:0, 1:1 or 1:2).

2.9. Equilibrium solubility of BCZ forms.

Six aqueous media were used to determine the equilibrium solubility of BCZ-FB, BCZHCl and $BCZH_2Cl_2$: ultrapure water, 0.01 mol L^{-1} HCl, 0.1 mol L^{-1} HCl, pH 4.5 acetate buffer (0.050 mol L^{-1}), pH 6.8 (0.072 mol L^{-1}) and pH 7.5 phosphate buffers (0.085 mol L^{-1}), according to Resolution Number 031/2010 and Technical Note Number 003/2013 (ANVISA, 2013). Previously sieved amounts (particle size from 200 mesh (75 μm) to 270 mesh (53 μm) using a BerTel™ granulometric analysis sieves, Brazil) of the three BCZ forms were individually added in flasks (n = 3) containing 4 mL of each medium and vortexed for 1 min until the saturation of these solutions. Subsequently, the flasks, protected from light, were agitated at 150 rpm and at 25 °C, using an IKA™ orbital shaker table, model Ks 501 digital (Switzerland). After 72 h of stirring, the samples were filtered through a nylon syringe filter (0.45 μm, ValuPrep 25 mm, Pall) and diluted properly in a mobile phase (methanol:water 4:1 v:v, pH 2.6). The amount of the three forms in each media was determined using a validated stability-indicating HPLC method (Kuminek et al., 2012), which was partially validated (selectivity, linearity, accuracy and precision) in this work (Figures S2 and S3 and Tables S1-S4, Supplementary material) according to the

Resolution RDC No. 166 of 2017 (ANVISA, 2017). The HPLC measurements were performed on an Agilent™ model HP1200 HPLC (USA) using a Waters™ X bridge C18 (150 × 4.6 mm-5 μm) column. The solubility of BCZ forms was statistically compared, using the ANOVA test with 95% of confidence. When the p-value is less than 0.05, the samples are considered different. The pH of the saturated solutions was measured before and after the stirring period. The remaining solid was separated from the supernatant and dried in a desiccator containing silica for 7 days. Thereafter, it was evaluated by PXRD to verify whether the resulting material was the same as the starting material.

2.10. Production of BCZ tablets with different BCZ forms

Three batches containing 60 tablets each were prepared to evaluate whether there is difference in solubility and dissolution between the three formulations: batch 1 (containing BCZ-FB), batch 2 (containing BCZHCl) and batch 3 (containing $BCZH_2Cl_2$). First, the placebos (inactive ingredients) were prepared using the following composition: microcrystalline cellulose (33.9%), lactose monohydrate (33.9%), starch (29.8%), povidone K30 (1.4%) and magnesium stearate (1.0%). Then, the amount of each BCZ form (particle size from 200 mesh to 270 mesh) was based on the proportion of BCZ in commercial oral solid dosages which contain 25 mg of its dihydrochloride solid modification: BCZ-FB (21.5 mg), BCZHCl (23.5 mg) and $BCZH_2Cl_2$ (25.0 mg). These ingredients were slowly mixed in an aluminum container for five minutes. The equivalent of an average weight (320 mg) of each formulation was weighed into a single rotary tablet compression machine Lemaq™ model LM08B (Brazil), which was used to produce the tablets (n = 60) by direct compression.

All of the prepared formulations contain the same average weight and excipients as Buclina®, the reference medicine of Sanofi Pharmaceutical industry. Additionally, the proportion of excipients was based according to the percentage used in the production of solid dosage forms (Aulton, 2016).

The compression strength used to produce all tablets was the same (4.2 Kgf). The reference value adapted to the strength was 4.0 to 4.5 Kgf. Determination of average weight, friability, assay and uniformity of the tablets were also determined according to USP 40 (USP, 2017). (Tables S5 –S9, Supplementary material).

2.11. Dissolution profile of BCZ tablets with different BCZ forms

The solubility analysis was the starting point to choose the ideal dissolution medium (pH 4.5 sodium acetate buffer) for the dissolution profile analysis. The dissolution profile of each formulation was performed in an Dissolutor Sotax™ model AT 7smart, multi-bath (n = 8) (apparatus II) (Switzerland), using a previously developed and validated method (Kuminek et al., 2012), with the following conditions: 900 mL of pH 4.5 sodium acetate buffer + 1.0% sodium lauryl sulfate at 37.0 ± 1.0 °C, apparatus II (paddle) and rotation of 75 rpm. Aliquots of 5 mL were collected from each vessel (n = 6), at sampling times of 5, 10, 15, 20, 30 and 60 min, followed by the immediate replacement of identical volumes of dissolution medium. The aliquots were filtered directly into vials using a 0.45 μm nylon syringe filter (0.45 μm, ValuPrep 25 mm, Pall) . The amount of dissolved buclizine at each sampling time was determined by HPLC method chromatography at a wavelength of 230 nm according to a validated method (Figures S2 and S4 and Tables 10 and 11, Supplementary material).

The similarity of the dissolution profiles was determined by the similarity factor (*f2*) calculated as follows:

$$f2 = 50xlog\left\{\left[1 + \left(\frac{1}{n}\right)\sum_{t=1}^{n}(Rt - Tt)^2\right]^{-0.5} x100\right\}$$

Where, n is the number of selected time points, Rt is the cumulative percentage dissolved at each of the selected n time points of the reference product, and Tt is the cumulative percentage dissolved at each of the selected n time points of the test product. The factor f2 measures the closeness between the two dissolution profiles, and values between 50 and 100 indicate similarity between two profiles (FDA, 1997).

3. Results and Discussion

3.1. Single-Crystal X-ray diffraction Analysis

3.1.1. Chiral molecules crystal packing types

Optical rotation measurements performed here confirm that raw material is a racemic mixture. Therefore, BCZ can adopt crystal packing types as follows: a racemic compound with a 1:1 stoichiometry (occurrence, 90–95%); a mechanical mixture (conglomerate) of single crystals containing only homochiral molecules (5–10%); and a solid solution crystal containing an equal number of enantiomers in a random distribution (less than 1%) (Deb et al, 2015). Since chiral molecules cannot be superimposed on an image of themselves created by the action of a mirror, center of inversion or an improper rotation axis, crystals containing only one enantiomer must adopt a non-centrosymmetric chiral structure (type NC) associated with point groups 1, 2, 222, 4, 422, 3, 32, 6, 622, 23 and 432. This rule also applies to conglomerates. On the other hand, achiral molecules can crystallize as an NC structure as well as a centrosymmetric achiral structure (type CA) associated with point group containing inversion center or non-centrosymmetric achiral structure (type NA) associated with a point group without an inversion center but containing a mirror and/or improper rotation axis. Finally, for racemic compounds and solid solution crystals, beyond the NC, there are also CA and NA types (Deb et al, 2015). Considering only racemic compounds, the frequency of CA, NA and NC are ~ 95%, 4.5–5% and ~ 0.02%, respectively (Deb et al, 2015).

Here, the $BCZHCl{\cdot}H_2O$ and BCZHCl structures were respectively solved in the space groups $Pca2_1$ and $Pna2_1$, where Cc and Pc together are the most predominant space groups of NA structures. The R-isomer, which is related to the S-isomer by the glide planes of $Pca2_1$ and $Pna2_1$, represents both BCZHCl and $BCZHCl{\cdot}H_2O$ asymmetric units (Fig. 1). The main crystallographic data for these are summarized in Table 1.

3.1.2. BCZHCl structure description

The BCZHCl structure presents one buclizine monocation ($BCLH^+$) and one chloride anion in the asymmetric unit. The protonation of the piperazine ring occurs at atom N2, which is the N atom that is most distant from the electronegative chlorophenyl moiety (Fig. 1a). The piperazine group (N1-C14-C15-N2-C16-C17) adopts a slightly distorted chair conformation with the puckering parameters Q, θ and φ of 0.598(6) Å, 175.7(5)° and 152(8)°. For an ideal chair conformation, the value of θ must be 0 or 180°. The substituents in BCZHCl (4-chlorodiphenylmethane and 1-methyl-4-*tert*-butylbenzene) occupy the equatorial positions of the piperazine ring. Selected torsion angles involving the piperazine ring and the substituents for BCZHCl compared to $BCZHCl{\cdot}H_2O$ are given in Table S12 (Supplementary material).

In the BCZHCl crystal packing (Figure S5, Supplementary material), the ion-pair is stabilized by a medium charge-assisted H-bond (Fig. 1a) involving the protonated N2 atom of the drug and the Cl^- anion (N2 − H2a•••Cl2). The ion-pairs are also connected to each other via two additional non-classical H-bonds (C13 − H13•••Cl2 and C17 − H17b•••Ct3) that contribute by linking the symmetry-related ion-pairs (where A and B are related by a glide plane perpendicular to the b-axis) into 1D chains (…A-B-A-B…) along the [1 0 0] direction (Fig. 2). These chains are themselves connected along the [0 1 0] direction through C15 − H15a•••Ct1 and C16 − H16b•••Ct2 H-bonds (Fig. 3a). In fact, the C − H•••π interactions (Fig. 3b) seem to fix the orientation adopted by the phenyl moieties, by reducing the rotation freedom around the C4-C7, C8-C7 and C18-C19 σ bonds. The overall 3D

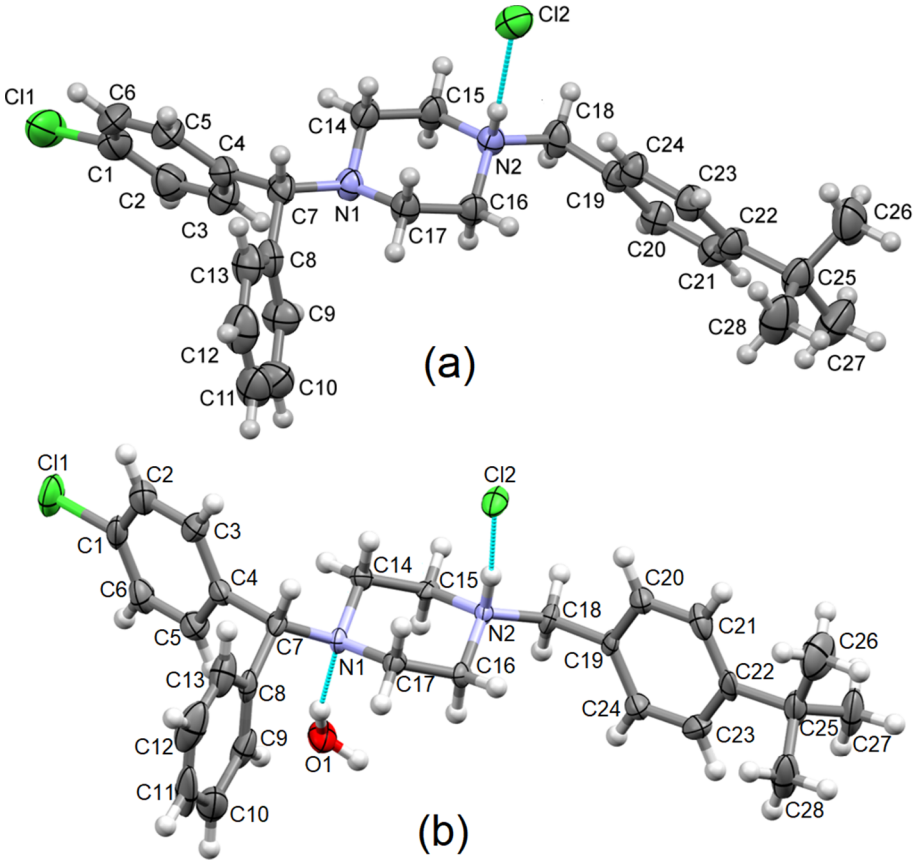

Fig. 1. ORTEP view of the asymmetric unit of BCZHCl (a) and BCZHCl·H_2O (b) structures at 293 and 150 K, respectively. Thermal ellipsoids for non-hydrogen atoms are drawn at a 50% probability level with the numbering scheme. Hydrogen bonds between the piperazine nitrogen atoms and chlorine counter-ion or water molecule are given in dashed cyan lines.

packing is also stabilized by non-classical H-bonds (C10 − *H*10•••Cl1) as well as other types of interactions (C − H•••H − C van der Waals contacts) (Figure S6, Supplementary material). The hydrogen bond geometries for BCZHCl are listed in Table 2.

3.1.3. *The BCZHCl·H_2O (150 K) structure description*

Contrary to our expectation of recrystallizing the raw material ($BCZH_2Cl_2$), the obtained single crystals were confirmed to be the monohydrochloride monohydrate salt (BCZHCl·H_2O). It is important to emphasize that the residual chloride quantification analysis show that raw material has twice the residual chloride value compared with BCZHCl and BCZHCl·H_2O forms, confirming the nominal API:counter-ion ratios (1:1 or 1:2).

In order to obtain a less disordered structure, the BCZHCl·H_2O dataset collected at 150 K was chosen for the structure description. The asymmetric unit comprises one buclizine monocation ($BCZH^+$), with the nitrogen N2 atom protonated, and one chloride anion as a counter-ion besides a water molecule (Fig. 1b). Also here, the piperazine ring adopts a distorted chair conformation, with the puckering parameters Q, θ, and φ of 0.573(6) Å, 177.0(6), and 220(14)°, respectively.

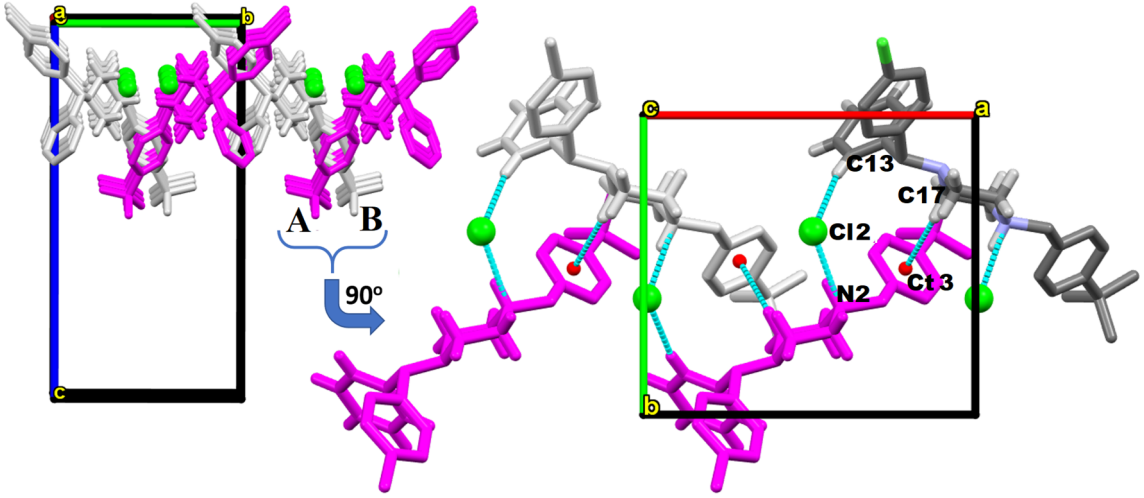

Fig. 2. View of the 1D chain along the [1 0 0] direction of the BCZHCl structure. The symmetry-related drug molecules are represented in white and magenta colors. The red spheres are centroids of the drug phenyl rings. The hydrogen bonds are represented by dashed cyan lines. The H atoms non-participating in the interactions have been omitted for clarity.

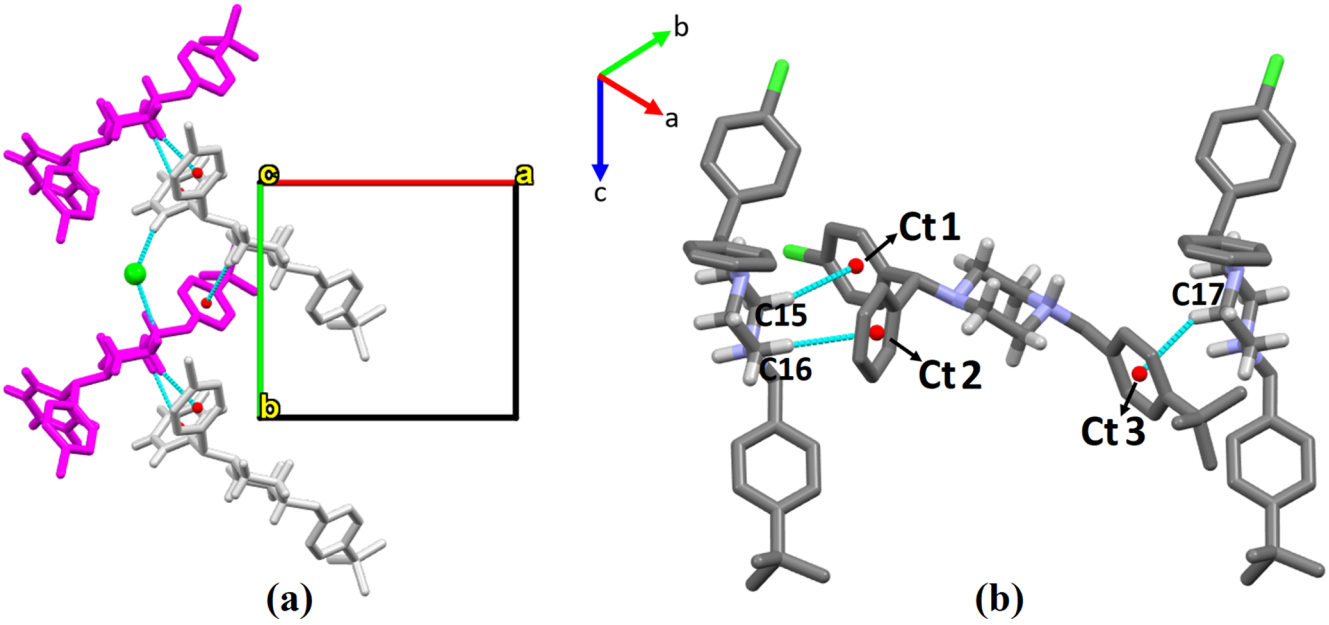

Fig. 3. View of the 2D hydrogen-bonded pattern depicting the non-classical C-H•••π interactions (dashed cyan lines) along the [1 0 0] direction (b). Detailed view of the inter-chain interactions (C-H•••π) in BCZHCl packing (b). Ct is the centroid of the drug phenyl rings. For clarity, only the H atoms involving in interactions are shown.

Table 2
Hydrogen bond geometry for BCZHCl, where D = Donor and A = Acceptor.

	Distance (Å)			Angle (°)	
Interaction	D···H	D…A	H…A	D-H…A	Symmetry code
N2 − H2a•••Cl2	0.98	3.012(4)	2.08	158	x, y, z
C13 − H13•••Cl2	0.93	3.735(8)	2.82	166	−1/2 + x, −1−y, z
C10 − *H*10•••Cl1	0.93	3.637(8)	2.87	141	+1/2−x, y, −1/2 + z
C15 − H15a•••Ct1	0.97	3.548(7)	2.72	143	1/2 + x, −y, z
C16 − H16a•••Ct2	0.97	3.942(6)	2.98	173	1/2 + x, −y, z
C17 − H17b•••Ct3	0.97	3.514(6)	2.83	128	−1/2 + x, −1−y, z

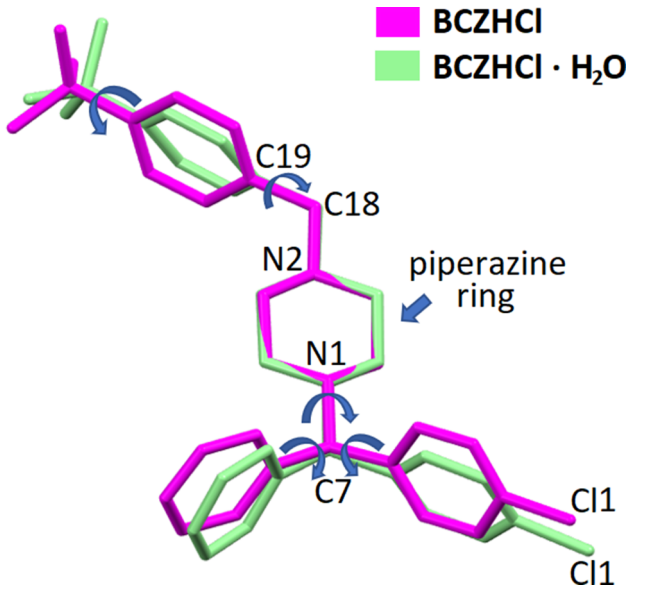

Fig. 4. Overlay of the backbones of BCZHCl and BCZHCl·H_2O isomers ((R)-isomers). The structures were matched considering all piperazine homologous non-hydrogen atoms using the Mercury structure overlay calculation (RMS Cartesian displacement = 0.032). For clarity, the hydrogen atoms were omitted.

Although the substituents in the BCZHCl·H_2O occupy the equatorial position of the piperazine ring, they show a conformational geometry that was slightly different from the corresponding isomer in the BCZHCl structure (Fig. 4 and Table S12, Supplementary material).

In the crystal, the protonated N2 atom acts as H-bond donor to the chloride anion, resulting in a medium charge-assisted H-bond (N2 − H2•••Cl2, Fig. 5). Since the chloride and water molecules are both intercalated between the drug molecules ($BCZH^+$), the ion-pair propagates by translation along the [0 0 1] direction through H-bonds involving the O1 atom as a H-bond donor and the chloride and piperazine N1 atoms as H-bond acceptors (Fig. 5).

The ion-pair is also stabilized by non-classical H-bonds between the chloride anion and the sp^3 carbon atoms, C16 and C18 of the drug (Fig. 5, Table 3). The drug molecules in these columnar stacks (Fig. 6a) interact with the drug molecules of the neighboring columns along the [0 1 0] direction by C-H•••π interactions (C27 − H27b•••Ct1 and C27 − H27c•••Ct2) (Fig. 6b). As in the anhydrous structure (BCZHCl),

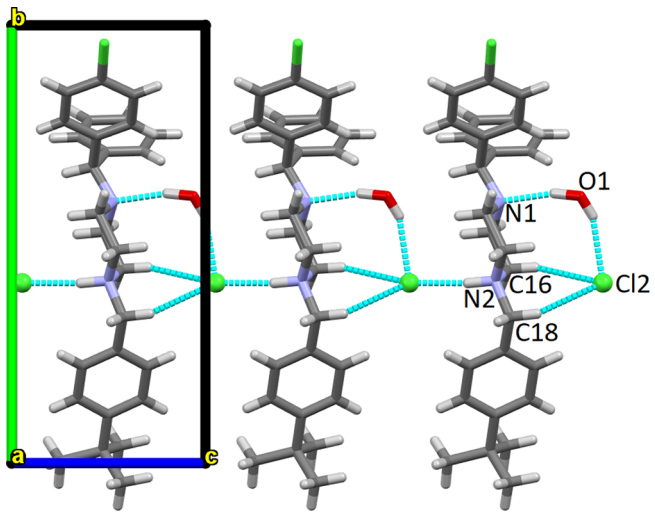

Fig. 5. Ionic chain along [0 0 1] direction additionally stabilized by water H-bonds and non-classical C-H···Cl interactions (depicted in dashed cyan lines).

Table 3
Geometric parameters of the BCZHCl·H_2O hydrogen bonds, where D = Donor and A = Acceptor.

	Distance (Å)			Angle (°)	
Interaction	D···H	D…A	H…A	D-H…A	Symmetry code
N2 – H2•••Cl2	0.98	3.067(6)	2.09	173	x, y, z
O1 – H1b•••N1	0.85(5)	2.904(8)	2.10(4)	159(7)	x, y, z
O1 – H1a•••Cl2	0.85(6)	3.205(5)	2.41(5)	157(7)	x, y, 1 + z
C16 – H16b•••Cl2	0.97	3.596(7)	2.72	151	x, y, 1 + z
C18 – H18b•••Cl2	0.97	3.607(8)	2.76	146	x, y, 1 + z
C27 – H27b•••Ct1	0.96	3.689(8)	2.73	173	x, −1 + y, z
C27 – H27c•••Ct2	0.97	3.712(9)	2.91	136	x, −1 + y, z

these interactions seem to fix the orientation adopted by phenyl moieties, by reducing the rotation freedom around the C4-C7, C8-C7 and C18-C19 σ bonds. The resulting 2D columnar layers pack along the [1 0 0] direction through van der Waals contacts (Fig. 7).

3.2. Characterization of the BCZ-FB, BCZHCl and $BCZH_2Cl_2$ bulk material

The experimental PXRD pattern of the powder raw material (Figure S7, Supplementary material) is equivalent to the experimental PXRD pattern of $BCZH_2Cl_2$ reported in the literature (Mostafa and Al-Badr, 2011). The experimental and calculated PXRD patterns of BCZHCl match well with each other, indicating that the raw material was completely converted to the BCZ monohydrochloride (Fig. 8). The experimental PXRD pattern of the BCZ-FB form differs from the PXRD patterns of the salts indicating that the molecular crystal was obtained. It was not possible to obtain a significant sampling of the powder corresponding to the BCZHCl·H_2O crystalline form, which restrained its characterization by other techniques.

The infrared spectra of the $BCZH_2Cl_2$, BCZHCl and BCZ-FB forms are shown in Fig. 9. The $BCZH_2Cl_2$ spectrum is similar to previously published (Mostafa and Al-Badr, 2011) spectra presenting characteristic peaks in the 3600–1500 cm^{-1} range at 3051 cm^{-1} (C–H stretch aromatic), 2961 cm^{-1} (C–H stretch aliphatic) and 2347 cm^{-1} (R_3–N^+–H stretch). Since tertiary amines do not absorb in the 3700–3100 cm^{-1} region, the broad peak at 3420 cm^{-1} viewed in the $BCZH_2Cl_2$ spectrum is probably due to sample moisture (Larkin, 2017; Silverstein and Webster, 2005). Indeed, tertiary amine salt groups are expected to show a broad and intense peak located in the range from 2770 to 2380 cm^{-1} assigned to an N^+–H stretching vibration (Thompson et al., 1965). Therefore, the broad band observed to either $BCZH_2Cl_2$ or BCZHCl with respective maximum intensity at 2347 cm^{-1} and 2326 cm^{-1} is the distinguishing feature of the salt form of BCZ relative to its free base. Additionally, it is observed that the intensity of the N^+–H stretch band is higher for $BCZH_2Cl_2$ than BCZHCl, taking the sharp peak at 2961 cm^{-1} as a reference. The difference in intensity could be correlated to the number of protonated piperazine nitrogen atoms (two in $BCZH_2Cl_2$ and one in BCZHCl) and could therefore be used to distinguish the two salt forms. Another notable difference between the salt forms is the band at 2806 cm^{-1} observed for BCZHCl only. Methylene groups next to the nitrogen atom in tertiary amines result in bands (doublets at slightly different frequencies) at ~ 2800 cm^{-1} which are absent from the $BCZH_2Cl_2$ spectrum due to the protonation of both piperazine nitrogen atoms (Auton, 2016). The protonation increases the C–H binding constant displacing these bands to a region of higher frequency, causing them to overlap with other bands expected for this spectral range (e.g., those ones at 3051 and 2961 cm^{-1}). However, when one of the piperazine nitrogen atoms became deprotonated in the BCZHCl form, and the characteristic shift in the C–H stretching of

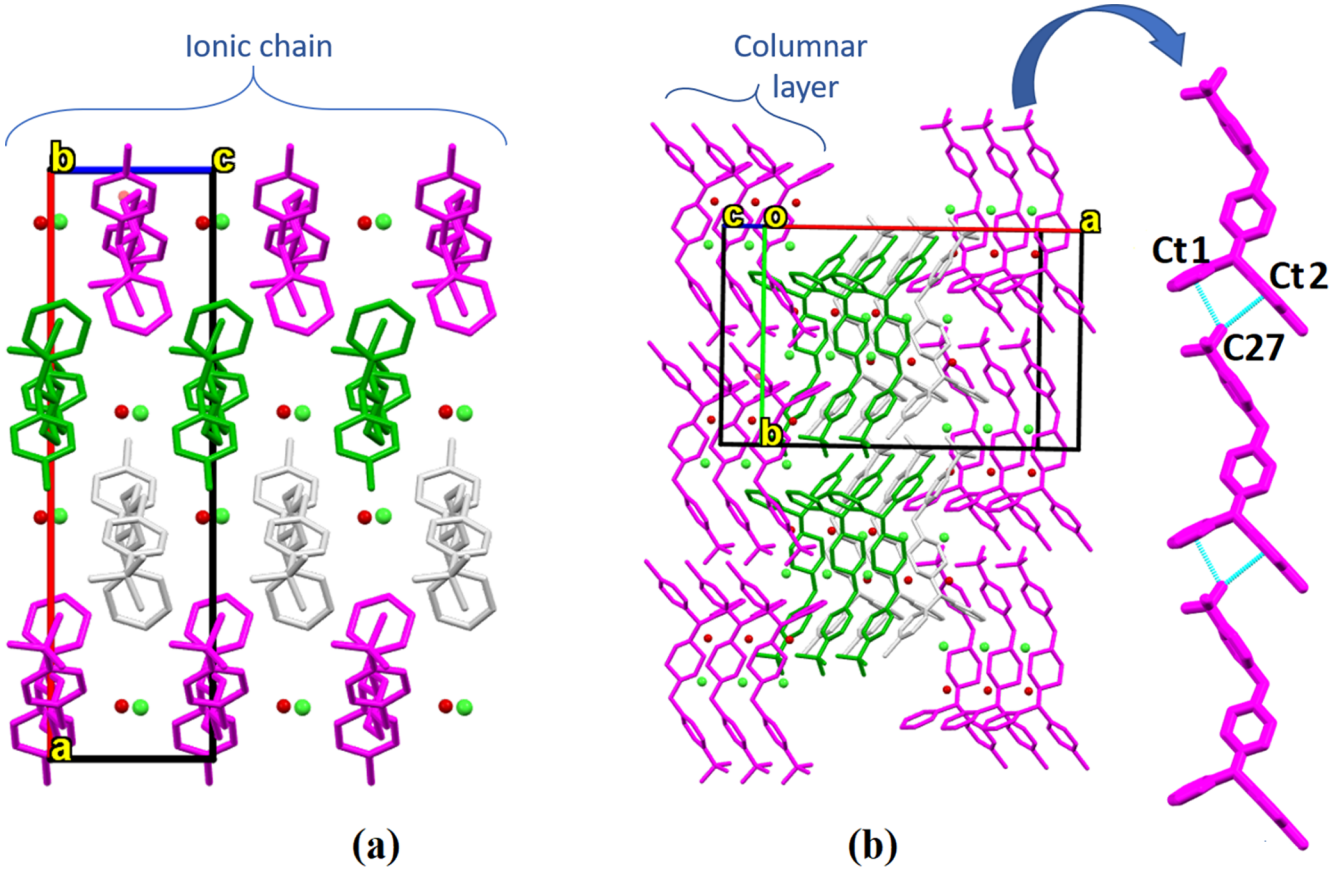

Fig. 6. View of the crystal packing onto *ac* (right) and *ab* (left) planes showing the columnar ionic chains (a) and columnar layers (b) along the [0 0 1] direction. The drug molecules related by symmetry operations are represented at the same color. Hydrogen atoms not involved in H-bonds were omitted for clarity.

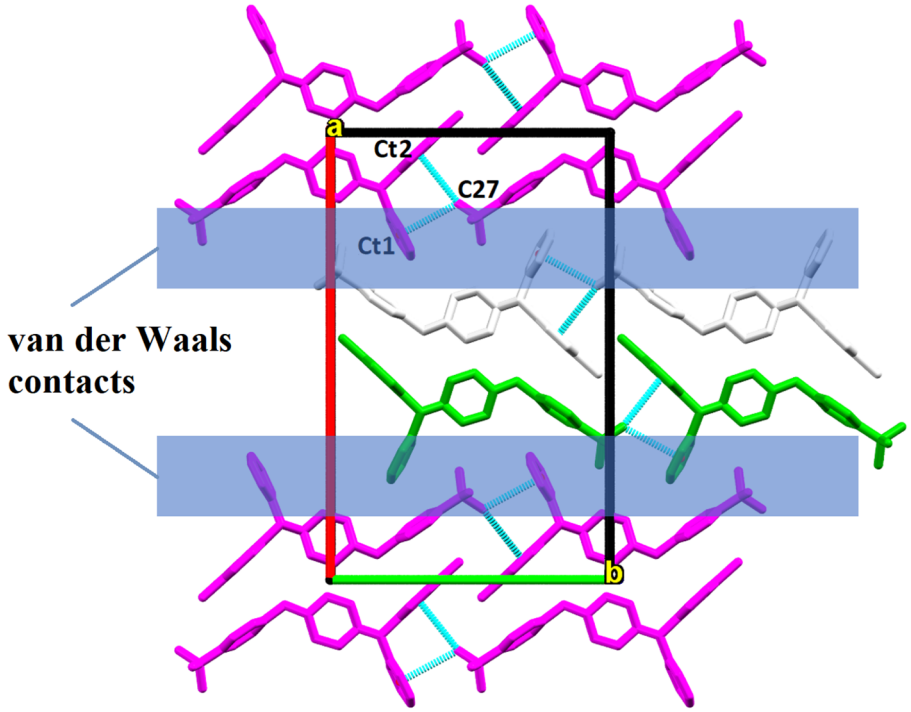

Fig. 7. View of the crystal packing onto the *ab* plane. The C-H···π H-bonds (dashed cyan lines) are responsible for linking the drugs along the [0 1 0] direction. The water molecules and also the hydrogen atoms non-participating of H-bonds were omitted for clarity.

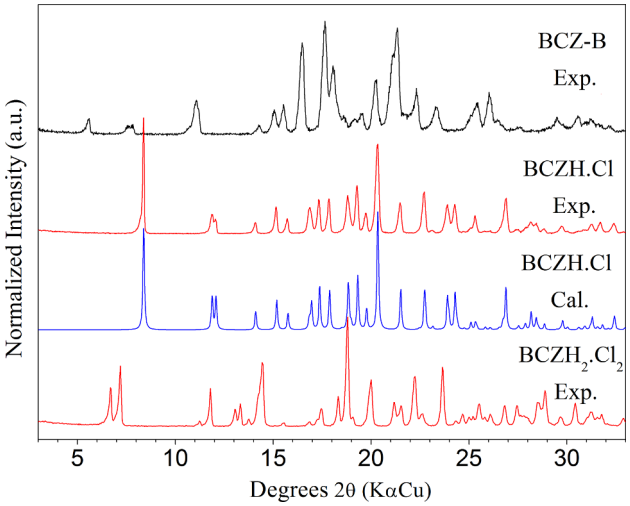

Fig. 8. Experimental PXRD patterns of $BCZH_2Cl_2$ (raw material), BCZ-FB and BCZHCl forms. The calculated PXRD pattern of BCZHCl was also included to ensure the purity of the BCZHCl powder sample.

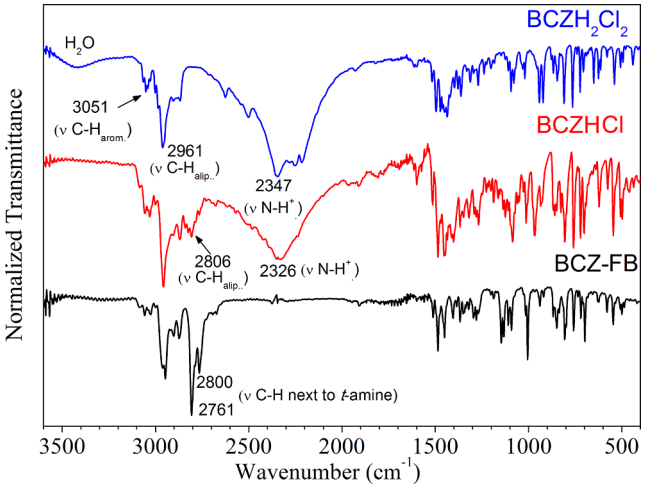

Fig. 9. IR spectra (in KBr pellet) of $BCZH_2Cl_2$, BCZHCl and BCZ-FB.

methylene groups next to tertiary amines was observed. As expected, the spectral changes were even more remarkable for BCZ-FB. The band attributed to the N^+–H stretch is completely absent, confirming that the two piperazine nitrogen atoms are deprotonated. Additionally, the double bands at 2800 and 2761 cm^{-1} (from C–H methylene groups next to tertiary amines) which are only observed in the BCZ-FB spectrum also confirms the deprotonation of both nitrogen atoms. In summary, the infrared spectroscopy analysis confirms the raw material as $BCZH_2Cl_2$ and the BCZ-FB crystallization for which the structural determination was not possible; this also enables us to differentiate the three BCZ solid modifications.

The DSC and TGA curves of $BCZH_2Cl_2$, BCZHCl and BCZ-FB are shown in Fig. 10. The complete DTA curves collected simultaneously to the TGA curves are shown in Figure S8 (Supplementary material). The $BCZH_2Cl_2$ DSC curve shows two endothermic peaks at 206 and 243 °C attributed to the beginning of its decomposition, since it is accompanied by a weight loss starting in the respective TGA curve (Fig. 10a). The weight loss of approximately 14.0% in the interval of 200–250 °C was attributed to the release occurring in two steps (highlighted by the DTG curve) of two HCl molecules (14.0%). The complete decomposition of $BCZH_2Cl_2$ is reached before 350 °C. The thermal behavior of the BCZHCl form is remarkably similar to that of $BCZH_2Cl_2$ (Fig. 10b). In spite of its 1:1 salt feature, the chloride amount (weight loss 7.0% corresponding to one HCl molecule, calc. = 7.0%) from the BCZHCl form is also released in two steps (DSC peaks at 227 and 240 °C). Indeed, the thermal decomposition similarity of the two salt forms is more clearly seen by the DTA curves (Figure S8, Supplementary material). The DSC curve of the BCZ-FB form shows a single endothermic peak at 105 °C corresponding to its melting (Fig. 10c). The TGA results show that the molten BCZ start its decomposition at ~ 250 °C which is

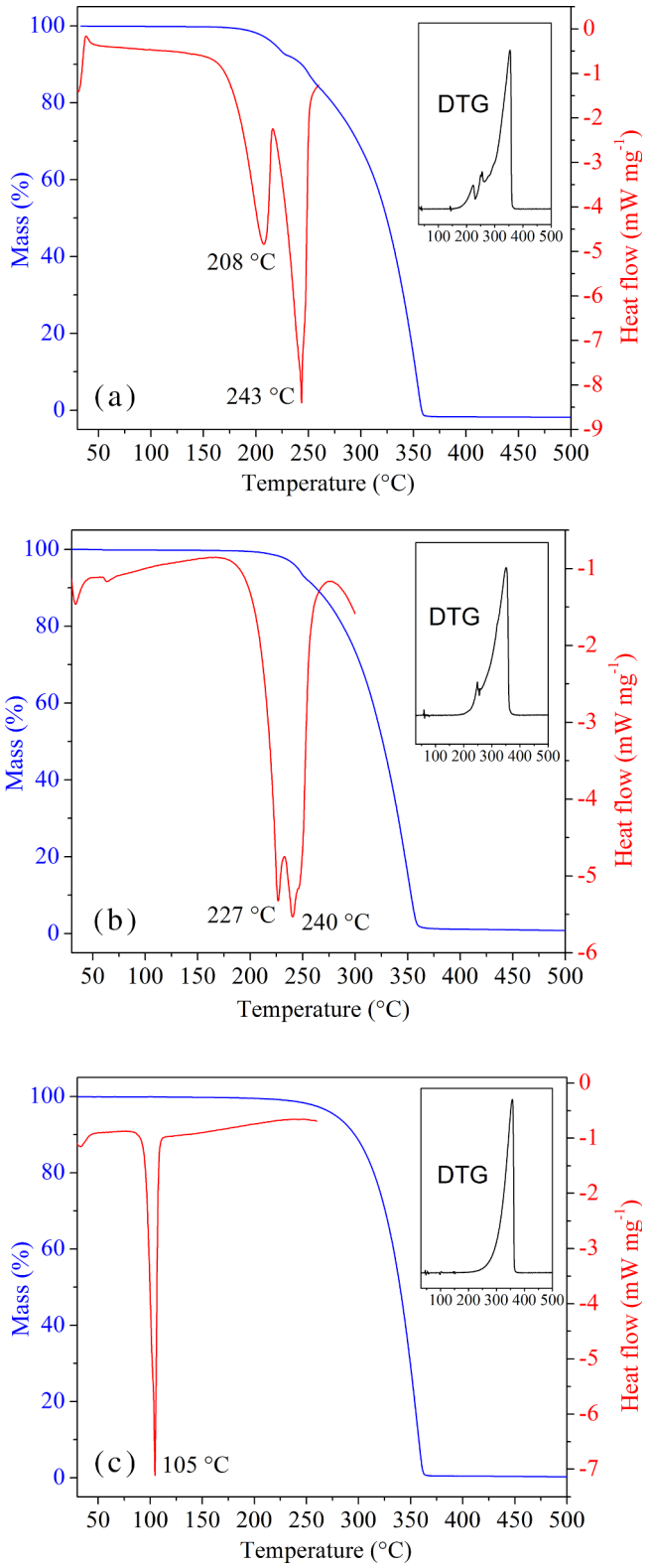

Fig. 10. DSC (in red) and TGA (in blue) curves for the (a) $BCZH_2Cl_2$, (b) BCZHCl and (c) BCZ-FB. The inset in the top right position is the TGA 1st derivative curve (DTG).

completed in a single step until 350 °C. In summary, the thermal analyses show signatures of the three forms and suggest a single-phase characteristic.

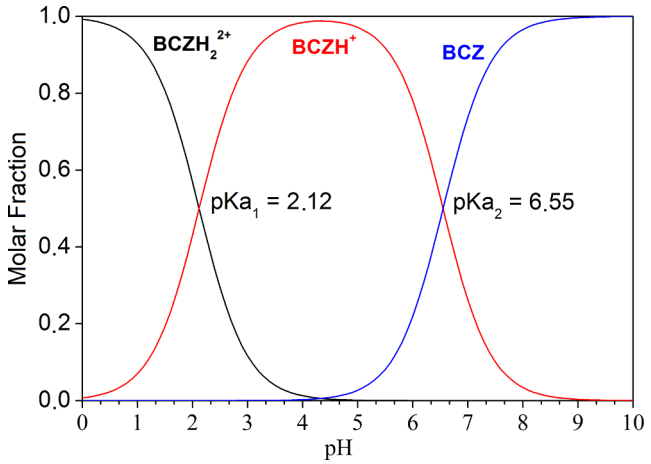

Fig. 11. The calculated pH-dependent acid − base BCZ species distribution. $\alpha_2 = [BCZH_2{}^{2+}]/C = (1 + (Ka_1/[H^+]) + (Ka_1 \times Ka_2/[H^+]^2))^{-1}$; $\alpha_1 = [BCZH^+]/C = \alpha_2(Ka_1/[H^+])$; $\alpha_0 = [BCZ^0]/C = \alpha_2(Ka_1 \times Ka_1/[H^+]^2)$; where $\alpha_0 + \alpha_1 + \alpha_2 = 1$ and $C = [BCZH_2{}^{2+}] + [BCZH^+] + [BCZ^0]$. Curves show pH in steps of 0.1.

3.3. Equilibrium solubility

Since BCZ is a weakly basic drug (weak electrolyte), its aqueous solubility is controlled by both the solution pH and the dissociation constant (pKa). However, to the best of our knowledge, neither experimental nor calculated dissociation constants associated with the protonation/deprotonation of the two BCZ piperazine nitrogen atoms ($BCZH_2{}^{2+} \overset{Ka1}{\leftrightarrow} BCZH^+ + H^+ \overset{Ka2}{\leftrightarrow} BCZ^0 + 2H^+$) have been published to date. Therefore, we used here the values (pKa1 = 2.12 and pKa2 = 6.55) calculated using the ChemSketch software from ACDLabs to sequentially calculate the pH-dependent acid-base BCZ species distribution (Fig. 11). It is important to mention that pKa1 refers to the N1 deprotonation, which is the piperazine nitrogen atom linked to the [(4-chlorophenyl) phenylmethyl] moiety (Scheme 2) as confirmed by the BCZHCl structure (item 3.1.2).

No significant variation was observed when comparing the equilibrium pH values (pH_f) with either the nominal (pH of the pure media) or starting (pH_i, measured immediately after placing the solid forms in contact with the media) pH values, except for the saturated solutions used to determine the equilibrium solubility of the two BCZ salt forms in ultrapure water pH = 6.8 and in 0.01 mol L^{-1} HCl medium (Table 4). The pH reduction for the BCZHCl (pH_f = 3.3) and $BCZH_2Cl_2$ (pH_f = 2.8) solutions using ultrapure water as medium was expected due to the hydrolysis of the cationic BCZ species released into the solution from these solid acidic salt forms.

Considering the 0.01 mol L^{-1} HCl media (pH_f from 1.9 to 2.9), the order of solubility was BCZ-FB > BCZHCl > $BCZH_2Cl_2$ (Fig. 12 and Table 4). This behavior was expected due to the probable formation of $BCZH_2{}^{2+}$ and/or $BCZH^+$ species in solution at pH less than 4.5 (Fig. 11). The lower solubility of BCZHCl and $BCZH_2Cl_2$ compared to BCZ-FB in HCl media could be attributed to the solubility suppression of the hydrochloride salt forms due to common ion effects. This hypothesis is reinforced by a reduction in the respective solubility values when the concentration of the HCl medium is increased to 0.1 mol L^{-1} (Fig. 12 and Table 4). It is also noted that the BCZ-FB > BCZHCl > $BCZH_2Cl_2$ trend is kept in the 0.1 mol L^{-1} HCl media (pH_f = 1.2). Therefore, the $BCZH_2Cl_2$ form (raw material) is the one that had the lowest solubility in the HCl media.

In ultrapure water medium, the BCZ-FB was insoluble (at least undetectable) and $BCZH_2Cl_2$ (final pH = 2.8) was more soluble than that of BCZHCl (final pH = 3.3) reversing the trend observed in the HCl media (Fig. 12 and Table 4). This result suggests that without the common ion effect, the balance of the exothermic process involving the

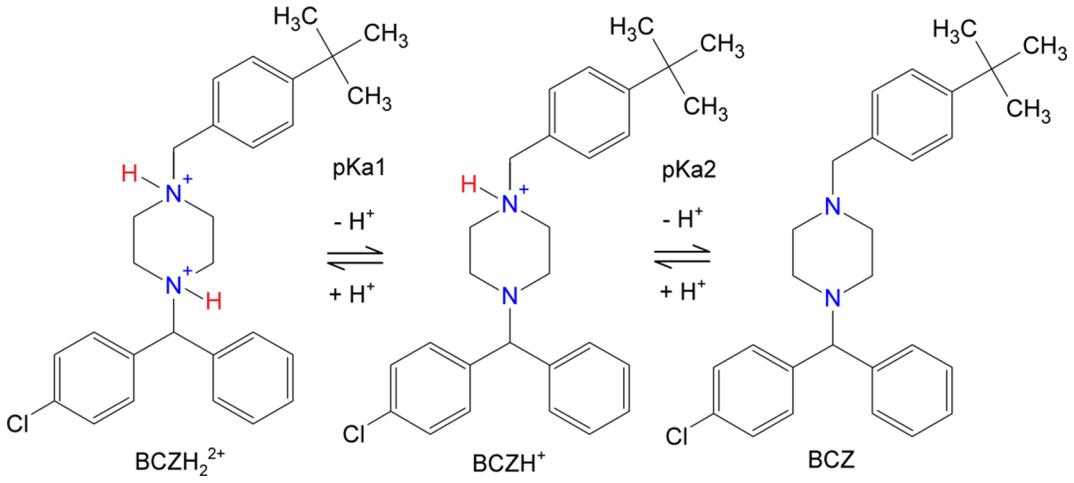

Scheme 2. pH-dependent BCZ species.

solvation of BCZ ionic/neutral species versus the endothermic process involving their release from the crystalline lattices, favors the $BCZH_2Cl_2$ solubility. In contrast to BCZHCl, the solubility of $BCZH_2Cl_2$ in water medium is higher than in both HCl media (Fig. 12 and Table 4).

The solubility trend observed in ultrapure water media ($BCZH_2Cl_2$ > BCZHCl > BCZ-$FB_{(insoluble)}$) is kept in acetate buffer pH 4.5 with a significant decrease in the solubility of the respective salt forms. However, since the solubility reduction of the BCZHCl form is more pronounced, the $BCZH_2Cl_2$ form became approximately 5-fold more soluble than the BCZHCl one (Fig. 12 and Table 4). It is also observed that the solubility of $BCZH_2Cl_2$ in acetate buffer pH 4.5 is comparable to those reached in the 0.1 and 0.01 mol L^{-1} HCl media. Finally, the three BCZ forms are insoluble in the pH 6.8 and pH 7.5 buffers, which is an expected behavior considering that the pH of these media are greater than the BCZ pKa2 (Figs. 11 and 12). The p-value of ANOVA evaluation was 0.0 (less than 0.05) for all forms, in the media HCl 0.01 mol L^{-1}, HCl 0.1 mol L^{-1}, sodium acetate pH 4.5 and water in a significance level of 5% showing that the three solid forms have distinct solubilities.

To be considered a class I or II in the BCS (Yu et al., 2002), the highest dosage of BCL (25 mg) must be soluble in 250 mL of aqueous media, which means reaching solubility values of at least 100 μg mL^{-1}. Since the solubility values found here are below this limit, the three BCZ forms should be classified as a class II (low solubility and high permeability) or IV (low solubility and low permeability) API.

The remaining solid material in equilibrium with the solutions used to determine the solubility of the crystal forms was analyzed by PXRD to determine whether the starting crystal forms are maintained during the equilibrium establishment. The PXRD patterns show that either $BCZH_2Cl_2$ or BCZHCl form remain as unique solid phase irrespective the media (Fig. 13 and Figures S9-S13, Supplementary material). On the one hand, our PXRD patterns also show that the BCZ-FB form is converted to the BCZHCl form during the establishment of equilibrium in the two media (0.1 and 0.01 mol L^{-1} HCl media) in which it was soluble (Fig. 13 and Figure S9, Supplementary material). The conversion occurs via protonation ($BCZ^0 + H^+ \rightarrow BCZH^+$) of the released neutral species from BCZ-FB, which is completely dissolved, followed by precipitation with the chloride ion from the HCl media. Because of this conversion, the BCZ-FB solubility in the HCl media cannot be considered actual values. As expected, in all media where the BCZ forms were insoluble (at least not detectable) no phase transition was observed (Figures S10-S13, Supplementary material).

3.4. Dissolution profile

Despite the higher and discriminative solubility values found for the BCZ forms in water and HCl media, the acetate buffer pH 4.5 medium was chosen for the dissolution profile assay performed here. The HCl media were discarded due to the BCZ-FB → $BCZH_2Cl_2$ phase transition observed during the establishment of equilibrium (Fig. 13 and Figure S6, Supplementary material), whereas the water medium was discarded due to the pH variation. The solubility results also indicated the need for surfactant addition to the chosen dissolution medium (ANVISA, 2013; Aulton, 2016) in order to reach the sink condition criteria (the dissolution profile assay considering the highest commercial dosage with 25 mg of $BCZH_2Cl_2$) (Table S13, Supplementary material). In order

Table 4
Equilibrium solubility (μg mL^{-1}) data for BCZ-FB, BCZHCl and $BCZH_2Cl_2$. The initial pH (pH_i) and final pH at the equilibrium (pH_f)* of each solution are also given.

	BCZ-FB	BCZHCl	$BCZH_2Cl_2$
0.1 mol L^{-1} HCl (pH = 1.0)	51.1 ± 1.9 pH_i = pH_f = 1.2	30.3 ± 1.1 pH_i = 1.1 pH_f = 1.2	12.2 ± 0.8 pH_i = 1.1 pH_f = 1.2
0.01 mol L^{-1} HCl (pH = 2.0)	75.7 ± 1.9 pH_i = 2.1 pH_f = 2.9	36.0 ± 3.1 pH_i = pH_f = 2.1	19.9 ± 1.2 pH_i = 2.4 pH_f = 1.9
Acetate buffer pH 4.5	ND[a] pH_i = pH_f = 4.5	3.1 ± 0.1 pH_i = pH_f = 4.5	16.3 ± 0.9 pH_i = pH_f = 4.5
Ultrapure water pH = 6.8	ND pH_i = 5.1 pH_f = 4.6	18.4 ± 0.7 pH_i = 3.9 pH_f = 3.3	34.8 ± 1.6 pH_i = 3.4 pH_f = 2.8
Phosphate buffer pH 6.8	ND pH_i = pH_f = 6.8	ND pH_i = pH_f = 6.8	ND pH_i = pH_f = 6.8
Phosphate buffer pH 7.5	ND pH_i = pH_f = 7.5	ND pH_i = pH_f = 7.5	ND pH_i = pH_f = 7.5

* After 72 h-stirring;
[a] ND = not detectable.

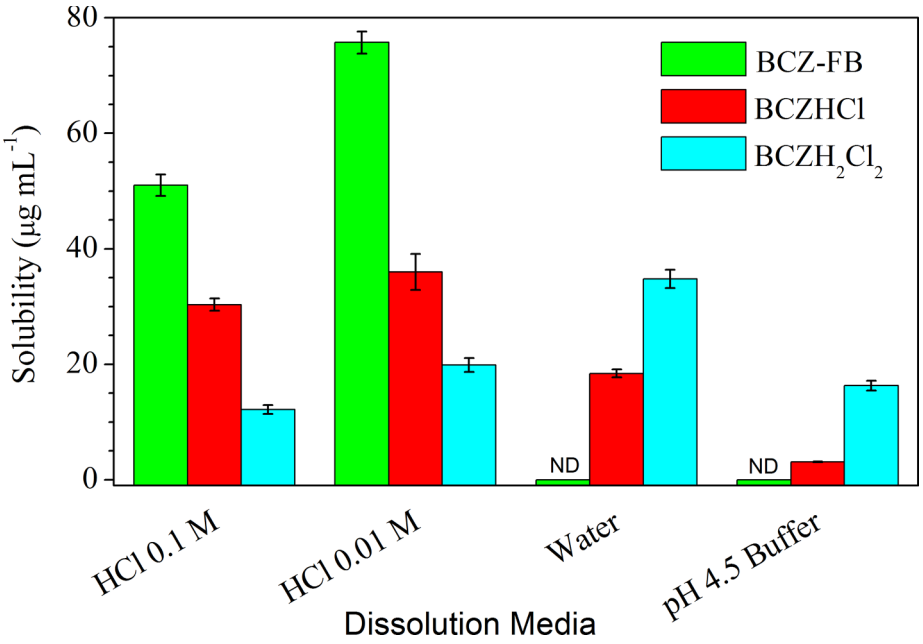

Fig. 12. pH-dependent equilibrium solubility values of BCZ-FB, BCZHCl, and $BCZH_2Cl_2$ (values and standard deviation in Table 4). ND = not detectable.

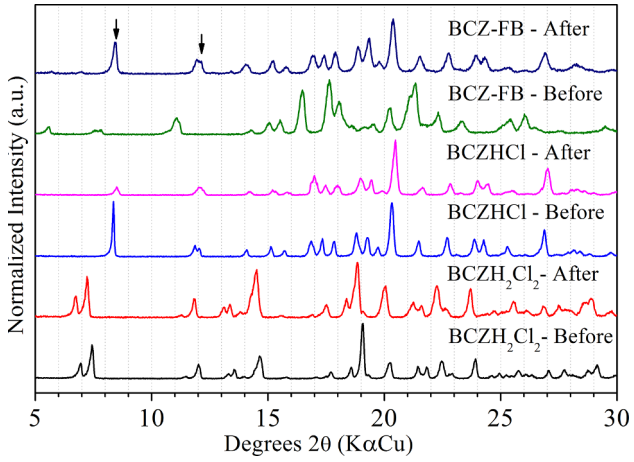

Fig. 13. Experimental PXRD patterns of $BCZH_2Cl_2$, BCZHCl, and BCZ-FB before and after the equilibrium solubility test in the 0.01 mol L^{-1} HCl medium.

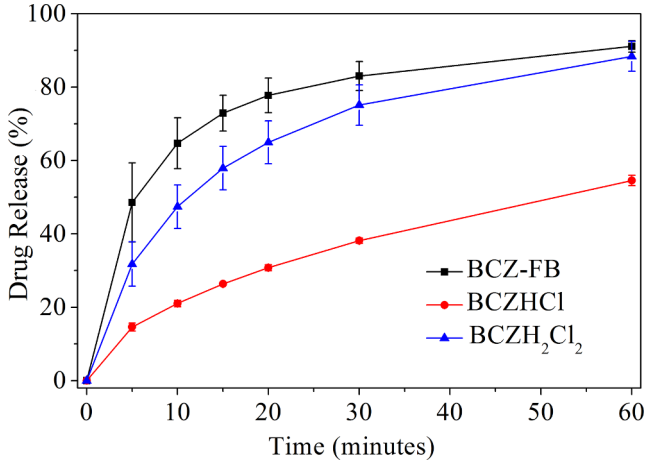

Fig. 14. Comparative dissolution profile between BCZ-FB, BCZHCl and $BCZH_2Cl_2$ in buffer pH 4.5 + 1.0% sodium lauryl sulfate dissolution medium.

to establish the smallest necessary amount of surfactant (FDA, 1997) to the dissolution profile assay, profiles containing 0.5 and 1.0% of sodium lauryl sulfate (SLS) were carried out for the $BCZH_2Cl_2$ form. The results (Table S14 and Figure S14, Supplementary material) led us to select the medium containing 1.0% of SLS due to its higher release rate (11.0% great than in the 0.5% SLS medium) and FDA guidance criteria (variation coefficient below 20% and 10% for the initial and final times, respectively) (FDA, 1997).

The comparative dissolution profile study using the optimized conditions was carried for the three BCZ forms (Fig. 14) reaching a dissolution percentage at 60 min of 91, 88, and 55% for BCZ-FB, $BCZH_2Cl_2$, and BCZHCl, respectively. The similarity factors (F2) calculated from the dissolution profiles (see item 2.9) are 44, 26, and 19 comparing $BCZH_2Cl_2$ vs. BCZ-FB, $BCZH_2Cl_2$ vs. BCZHCl, and BCZ-FB vs. BCZHCl, respectively. Therefore, all forms are different from each other in terms of performance because the three combinations have an F2 less than 50. The larger percentage of release for BCZ-FB could be attributed to a better interaction of the neutral species with the non-polar chains of SLS compared to the saline forms. In contrast to the salt forms, the BCZ-FB tablets have a high percentage of release, which could be due to a better interaction of neutral molecules with the non-polar chains of SLS.

4. Conclusions

Buclizine monohydrochloride monohydrate ($BCZHCl{\cdot}H_2O$) and its anhydrous form, BCZHCl, were solved and refined in the non-centrosymmetric space groups *P*na2_1 and *P*ca2_1, respectively. Since recrystallization of the raw material ($BCZH_2Cl_2$) resulted in $BCZHCl{\cdot}H_2O$ single crystals, the X-ray structure of $BCZH_2Cl_2$ was not determined. Efforts to solve the buclizine free-base (BCZ-FB) were hindered by weakly diffracting crystals, however, its existence was successfully confirmed by a series of techniques and by comparison of the obtained results with those found for the raw material and BCZHCl form. In the FT-IR spectrum, the vibrational mode relative to the piperazine N^+–H stretching was used to differentiate the buclizine salts from the free-base; the broad and intense peak seen in the salt's spectra at 2770–2380 cm^{-1} was absent in the BCZ-FB one. Also, for the salts, the DSC curves showed two endothermic peaks in the range of 200–250 °C corresponding to the decomposition process, whereas for the free-base,

there was only one peak at 105 °C due to melting. Moreover, the TGA profile of BCZ-FB was significantly different from the salts. In contrast to a single step process, the thermal degradation of $BCZH_2Cl_2$ and BCZHCl salts was characterized by two step events associated with the loss of two and one HCl molecules besides the drug itself, respectively.

As a result of protonation and the formation of $BCZH_2^{2+}$ and/or $BCZH^+$ species, BCZ-FB showed the highest solubility values in HCl media. On the other hand, due to the common ion effect, $BCZH_2Cl_2$ and BCZHCl salts showed the lowest ones. In ultrapure water medium, BCZ-FB was insoluble (at least undetectable) and $BCZH_2Cl_2$ was more soluble than BCZHCl, thus reversing the trend observed in HCl media. This trend ($BCZH_2Cl_2$ > BCZHCl > BCZ-FB (insoluble)) was also retained in acetate buffer pH 4.5 with a significant decrease of the respective solubility values.

The dissolution studies of BCZ-FB, BCZHCl and $BCZH_2Cl_2$ were performed in buffer pH 4.5 containing 1.0% of sodium lauryl sulfate (SLS). The most significant results were found for BCZ-FB (within 5 min, approximately 50% of the drug had been released) and were attributed to a better interaction of the neutral species with the non-polar hydrocarbon chains of SLS. Comparing the dissolution profile of the three forms, BCZ-FB, BCZHCl and $BCZH_2Cl_2$, we verified that BCZ-FB could be an alternative to replace $BCZH_2Cl_2$, since the latter presents as a major problem a solid-state conversion to its monohydrochloride monohydrate salt, $BCZHCl{\cdot}H_2O$ Additionally, other alternatives to avoid this anionic change passes by the development of new multi-component forms via cocrystallization of $BCZH_2Cl_2$ with other co-formers. However, even being an undesirable form, the identification and elucidation of $BCZHCl.H_2O$ structure, play a key role by providing an X-ray diffraction pattern useful for a fast and accurate industrial quality control (Atici and Karliga, 2015).

CRediT authorship contribution statement

Monalisa Bitencour: Conceptualization, Methodology, Formal analysis, Writing - original draft. **Olimpia Maria Martins Santos Viana:** Supervision, Methodology, Formal analysis, Writing - original draft. **Andre Luiz Machado Viana:** Methodology, Formal analysis, Writing - original draft. **Jennifer Tavares Jacon Freitas:** Methodology, Formal analysis, Writing - original draft. **Cristiane Cabral de Mel:** Software, Methodology, Formal analysis, Writing - review & editing. **Antonio Carlos Doriguetto:** Supervision, Writing - review & editing, Project administration, Funding acquisition.

Declaration of Competing Interest

The authors declare that they have no known competing financial interests or personal relationships that could have appeared to influence the work reported in this paper.

Acknowledgements

The authors acknowledge the Brazilian funding agencies FAPEMIG (PPM-00533-16 and APQ-01835-18), CNPq (428475/2018-3 and 308893/2019-0), FINEP (ref. 134/08) and CAPES (PNPD grant and finance Code 001) for financial support. We also thank CNPq (A.C.D.) and CAPES (M.B., J.T.J.F., and C.C.M.) for the research fellowships. We would like to express our sincere thanks to Professor Gislaine Ribeiro Pereira, the NCQ-UNIFAL-MG staff and Erik Respini, Simona Beretta, Leandro Checchinato, Emanuela Piga, Marco Trucco and all team of AS &T from NOVARTIS-Locarno-Switzerland for all facilities available. The authors gratefully acknowledge Dra. Charlane Cimini Correa from Federal University of Juiz de Fora for providing single crystal X-ray facilities.

Authorship

The manuscript was written through contributions of all authors. All authors have given approval to the final version of the manuscript. All authors contributed equally.

Appendix A. Supplementary data

Supplementary data to this article can be found online at https://doi.org/10.1016/j.ijpharm.2020.119840.

References

ACD/ChemSketch, 2018. Advanced Chemistry Development. Inc, Toronto, ON, Canada.
Agilent, 2010. Agilent Technologies UK Ltd, n.d, CrysAlisPRO. Oxford Diffraction.
Allen, F.H., 2002. The Cambridge structural database: a quarter of a million crystal structures and rising. Acta Crystallogr. Sect. B 58, 380–388. https://doi.org/10.1107/S0108768102003890.
Amidon, G.L., Lennernäs, H., Shah, V.P., Crison, J.R., 1995. A theoretical basis for a biopharmaceutic drug classification: the correlation of in vitro drug product dissolution and in vivo bioavailability. Pharm. Res. 12, 413–420. https://doi.org/10.1023/A:1016212804288.
ANVISA, 2013. Brazilian Health Regulatory Agency (ANVISA). Nota técnica no. 003/2013 [WWW Document]. URL http://portal.anvisa.gov.br/documents/33836/349757/Nota+t%C3%A9cnica+n%C2%BA+03+de+2013+-+CEFAR-GTFAR-GGMED-Anvisa/2c769030-a303-4c8f-adc8-5fd781695725 (accessed on Sep 09, 2020).
ANVISA, 2017. Brazilian Health Regulatory Agency (Anvisa). RDC Nº 166 [WWW Document]. URL https://pesquisa.in.gov.br/imprensa/jsp/visualiza/index.jsp?jornal=1&data=25/07/2017&pagina=87 (accessed on Feb 15, 2019).
Atici, E.B., Karliga, B., 2015. Quantitative determination of two polymorphic forms of imatinib mesylate in a drug substance and tablet formulation by X-ray powder diffraction, differential scanning calorimetry and attenuated total reflectance Fourier transform infrared spectroscopy. J Pharm Biomed Anal. 114, 330–340. https://doi.org/10.1016/j.jpba.2015.06.011.
Aulton, M.E., 2016. Delineamento de formas farmacêuticas, 4th ed. Rio de Janeiro.
Babu, T., 2011. Buclizine is back again! This time as a pediatric appetite stimulant. Indian J. Pharmacol. 43, 219. https://doi.org/10.4103/0253-7613.77383.
Beckmann, W., 2013. Crystallization: Basic Concepts and Industrial Applications. Wiley-VCH, 360p.
Cianci, M., Helliwell, J.R., Helliwell, M., Kaucic, V., Logar, N.Z., Mali, G., Tusar, N.N., 2005. Anomalous scattering in structural chemistry and biology. Crystallogr. Rev. 11, 245–335. https://doi.org/10.1080/08893110500421268.
Conklin, F.J., Nesbitt, R.E.L., 1958. Buclizine Hydrochloride for Nausea and Vomiting of Pregnancy. Obs. Gynecol 11, 214–219.
Cruz-Cabeza, A.J., 2012. Acid–base crystalline complexes and the pKa rule. CrystEngComm. 14, 6362–6365. https://doi.org/10.1039/c2ce26055g.
De Melo, C.C., Da Silva, C.C.P., Pereira, C.C.S.S., Rosa, P.C.P., Ellena, J., 2016. Mechanochemistry applied to reformulation and scale-up production of Ethionamide: Salt selection and solubility enhancement. Eur. J. Pharm. Sci. 81, 149–156. https://doi.org/10.1016/j.ejps.2015.10.007.
Deb, J., Majumder, J., Dastidar, P., Husain, A., Jana, S.S., 2015. Cetirizine derived supramolecular topical gel in action: rational design, characterization and in vivo self-delivery application in treating skin allergy in mice. J. Mater. Chem. B 3, 6634–6644. https://doi.org/10.1039/c5tb00676g.
FDA, 1997. Dissolution Testing of Immediate Release Solid Oral Dosage Forms. Guidance for Industry.
FDA, 2017. Waiver of In vivo Bioavailability and Bioequivalence Studies for Immediate – Release Solid Oral Dosage Forms Based on a Biopharmaceutics Classification System. Guidance for Industry.
Flack, H.D., 1983. On enantiomorph-polarity estimation. Acta Crystallogr. Sect. A 39, 876–881. https://doi.org/10.1107/S0108767383001762.
Flack, H.D., 2003. Chiral and achiral crystal structures. Helv. Chim. Acta 86, 905–921. https://doi.org/10.1039/a908985c.
Gao, Z., Rohani, S., Gong, J., Wang, J., 2017. Recent Developments in the Crystallization Process: Toward the Pharmaceutical Industry. Engineering 3, 343–353. https://doi.org/10.1016/J.ENG.2017.03.022.
Mostafa, G.A.E., Al-Badr, A.A., 2011. Buclizine: Profiles of Drug Substances, Excipients and Related Methodology 1st ed. Elsevier Inc., Riyadh. 36:1-33. https://doi.org/10.1016/B978-0-12-387667-6.00001-4.
Hooft, R.W.W., Straver, L.H., Spek, A.L., 2008. Determination of absolute structure using Bayesian statistics on Bijvoet differences. J. Appl. Cryst. 41, 96–103. https://doi.org/10.1107/S0021889807059870.
Hooft, R.W.W., Straver, L.H., Spek, A.L., 2010. Using the *t*-distribution to improve the absolute structure assignment with likelihood calculations. J. Appl. Cryst. 43, 665–668. https://doi.org/10.1107/S0021889810018601.
Kuminek, G., Stulzer, H.K., Tagliari, M.P., Oliveira, P.R., Bernardi, L.S., Rauber, G., Cardoso, S.G., 2012. Development and Validation of a Stability-Indicating HPLC Method for the Determination of Buclizine Hydrochloride in Tablets and Oral Suspension and its Application to Dissolution Studies. Quim. Nov. 35, 207–212. https://doi.org/10.1590/S0100-40422012000100036.
Larkin, P., 2017. Infrared and Raman Spectroscopy: Principles and Spectral

Interpretation, 2nd ed. .
Mitchell, A.G., 1998. Racemic Drugs: Racemic Mixture, Racemic Compound, or Pseudoracemate? J. Pharm. Pharm. Sci. 1, 8–12.
Mohanty, S., Reddy, S.G., Ramadevi, B., Karmakar, A.C., 2015. An assembly of structurally diverse small and simple 5-aminomethylene derivatives of 2,4-thiazolidinedione and studies of their biological activity. Med. Chem. Res. 24, 4037–4049. https://doi.org/10.1007/s00044-015-1447-0.
Parsons, S., Flack, H., 2004. Precise absolute-structure determination in light-atom crystals. Acta Crystallogr. Sect. A Found. Crystallogr. A 60, s61. https://doi.org/10.1107/s0108767304098800.
Peraman, R., Manikala, M., Kondreddy, V.K., Yiragamreddy, P.R., 2015. A stability-indicating RP-HPLC method for the quantitative analysis of meclizine hydrochloride in tablet dosage form. J. Chromatogr. Sci. 53, 793–799. https://doi.org/10.1093/chromsci/bmu127.
Silverstein, R.M., Webster, F.X., 2005. Spectrometric Identification of Organic Compounds, 7th ed.
Savjani, K.T., Gajjar, A.K., Savjani, J.K., 2012. Drug Solubility: Importance and Enhancement Techniques. ISRN Pharm. 2012, 1–10. https://doi.org/10.5402/2012/195727.
Serajuddin, A.T.M., 2007. Salt formation to improve drug solubility. Adv. Drug Deliv. Rev. 59, 603–616. https://doi.org/10.1016/j.addr.2007.05.010.
Sheldrick, G.M., 2015. Crystal structure refinement with SHELXL. Acta Crystallogr. Sect. C Struct. Chem. 71, 3–8. https://doi.org/10.1107/S2053229614024218.
Song, Y., Chidan Kumar, C.S., Akkurt, M., Chandraju, S., Li, H., 2012. 1-[(4-Chlorophenyl)(phenyl)methyl]piperazine-1,4-diium bis- (trichloroacetate)-trichloroacetic acid (1/1). Acta Crystallogr. Sect. E Struct. Reports Online E68, o2695–o2696. https://doi.org/10.1107/S1600536812034794.
Spek, A.L., 2009. Structure validation in chemical crystallography. Acta Crystallogr. Sect. D 65, 148–155. https://doi.org/10.1107/S090744490804362X.
Thompson, W.E., Warren, R.J., Eisdorfer, I.B., Zarembo, J.E., 1965. Identification of primary, secondary, and tertiary pharmaceutical amines by the infrared spectra of their salts. J. Pharm. Sci. 54, 1819–1821. https://doi.org/10.1002/jps.2600541231.
USP, 2017. U.S. Pharmacopeia National Formulary 2017: USP 40 NF 35.
Watcha, M.F., 2002. Postoperative nausea and emesis. Anesthesiol. Clin. N. Am 20, 709–722. https://doi.org/10.1016/S0889-8537(02)00010-X.
Yu, L.X., Amidon, G.L., Polli, J.E., Zhao, H., Mehta, M.U., Conner, D.P., Shah, V.P., Lesko, L.J., Chen, M.-L., Lee, V.H.L., Hussain, A.S., 2002. Biopharmaceutics classification system: the scientific basis for biowaiver extensions. Pharm. Res. 19, 921–925. https://doi.org/10.1023/A:1016473601633.